EVALUATING THE EFFECT OF SUPER FINISHING ON GEARS

Sriram Sundar, Dr. Jason Dreyer, Dr. Rajendra Singh

Abstract

The aim of this study is to evaluate the effect of super finishing on gear acceleration and noise level. Many researchers [1-13] have studied the gear dynamic models to study the effect of various parameters on gear dynamics. A 6DOF model is developed and experimental studies were conducted. In this study, the effects of super finishing [14, 15] on gear acceleration and noise level were evaluated at various torques, speeds and temperatures. Experimental measurements were made at KAC on single mesh spiral bevel gear box (from two tail rotor gear boxes of a SH-2 SeaSprite helicopter, both with a significant number of flight hours and one with reconditioned super finished gear surfaces). The gear box casing acceleration and sound pressure radiated from the gear box were measured. The values predicted from the extended model and the experimental values were compared in frequency domain at the calculated gear mesh harmonics. The 6DOF model developed is a spur model [18, 19], modified to be representative of the spiral bevel gear system. This conceptual model is used to suggest explanations for trends observed in the experimental data. Analysis of variance (ANOVA) of the experimental and modeling results was used to identify and compare statistically significant trends.

1. 6DOF model to predict the effect of super finishing

The 6DOF linear time-varying (LTV) model of a spur gear pair used is shown in the schematic in Fig 1. Here, $h_p(t)$ and $h_g(t)$ represent prescribed teeth surfaces with respect to ideal involute profiles of pinion (subscript p) and gear (subscript g) respectively.

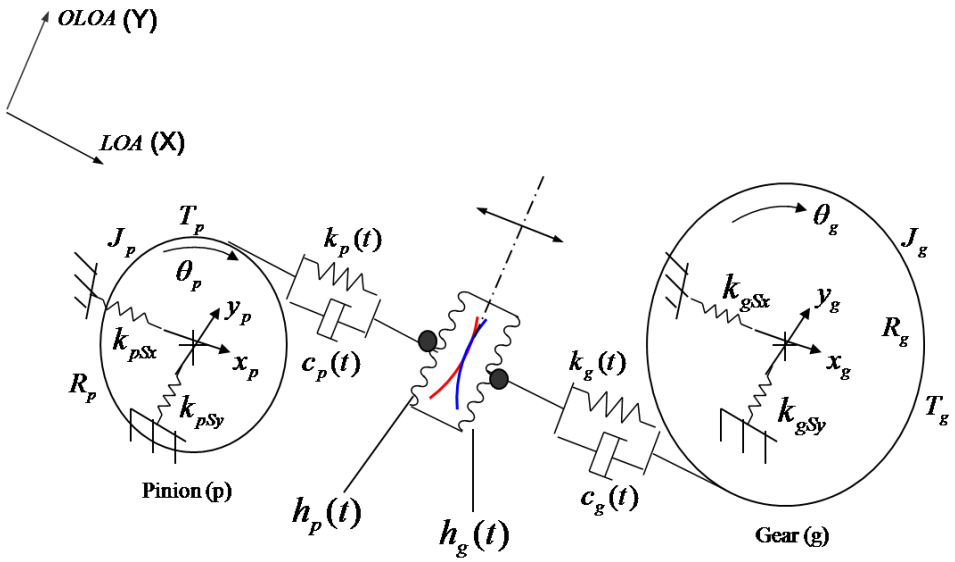

Fig.1: Proposed 6DOF linear time-varying gear dynamics model with prescribed tooth surface undulations $h_p(t)$ and $h_g(t)$. Here LOA is the line-of-action (X) and OLOA is the off-line-of-action (Y) direction.

Sinusoidal, periodic and random tooth surface undulations are examined. In this model, the undulation amplitude is independent of the load though an equivalent loaded static transmission error is also calculated. The static transmission error, surface undulation and sliding friction are assumed as simultaneous excitation. The system is governed by torsional motions $\theta_p(t)$ and $\theta_g(t)$ and translational motions along the LOA (X) direction (xp(t), xg(t)) and the OLOA (Y) direction ($y_p(t)$, $y_g(t)$). Here, J_p and J_g are the polar moments of inertia and Tp and Tg are the external and braking torques; R_p and R_g are base radii; k_{pSx} and k_{gSx} are the effective shaft-bearing stiffness in the X direction, and k_{pSy} and k_{gSy} are the effective shaft-bearing stiffness in the Y direction. Though the acceleration predictions can be made from both LTI and LTV systems, only the results from LTV system are used based on the results from the previous chapter. For this model mesh stiffness ($k_p(t)$ and $k_g(t)$), moment arms ($X_p(t)$ and $X_g(t)$) and coefficient of friction ($\mu(t)$) vary with the roll angle (α) and thus with time (t). The $k_p(t)$ and $k_g(t)$ variations are calculated,

over a range of one mesh cycle T, by using gear contact mechanics codes such as the Load Distribution Program (LDP) [16] and Calyx software [17].

1.1 Equations of motion for the 6DOF LTV model

With reference to the system shown in Fig. 1, the governing equations for torsional motions $\theta_p(t)$ and $\theta_g(t)$ are:

$$J_p\ddot{\theta}_p(t) = T_p + \sum_{i=0}^{n} X_{pi}(t)F_{pfi}(t) - \sum_{i=0}^{n} R_p N_{pi}(t) \tag{1}$$

$$J_g\ddot{\theta}_g(t) = -T_g + \sum_{i=0}^{n} X_{gi}(t)F_{gfi}(t) + \sum_{i=0}^{n} R_g N_{gi}(t) \tag{2}$$

The time-varying moment arms $X_{pi}(t)$ and $X_{gi}(t)$ for the i^{th} meshing pair with a σ contact ratio are:

$$X_{pi}(t) = L_{XA} + (n-i)\lambda + \mathrm{mod}(\Omega_p R_p t, \lambda) \tag{3a}$$

$$X_{gi}(t) = L_{YC} + i\lambda - \mathrm{mod}(\Omega_g R_g t, \lambda) \tag{3b}$$

Where, n = floor(σ) in which the "floor" function rounds off the σ to the nearest integer (towards a lower value); mod(x, y) = x – y ·floor(x/y) is the modulus function, if y≠0; Ωp and Ωg are the nominal speeds (in rad/s); and LAP, LXA and LYC are the geometric length constants. The normal loads $N_{pi}(t)$ and $N_{gi}(t)$ are defined as follows:

(4)

where $k_i(t)$ and $c_i(t)$ are time-varying mesh stiffness and viscous damping coefficients for the ith meshing pair. The instantaneous sliding friction forces $F_{pfi}(t)$ and $F_{gfi}(t)$ in terms of $\mu(\tau)$ for the i^{th} meshing pair are:

$$F_{pfi}(t) = \mu_i(t) N_{pi}(t), \qquad F_{gfi}(t) = \mu_i(t) N_{gi}(t) \tag{5 a,b}$$

In the equations 4 and5 (a, b) the surface undulation, static transmission error and sliding friction are considered as excitations simultaneously.

The governing equations for translations $x_p(t)$ and $x_g(t)$ motions in the X direction are:

$$m_p \ddot{x}_p(t) + 2\zeta_{pSx}\sqrt{k_{pSx} m_p}\,\dot{x}_p(t) + k_{pSx} x_p(t) + \sum_{i=0}^{n} N_{pi}(t) = 0 \tag{6}$$

$$m_g \ddot{x}_g(t) + 2\zeta_{gSx}\sqrt{k_{gSx} m_g}\,\dot{x}_g(t) + k_{gSx} x_g(t) + \sum_{i=0}^{n} N_{gi}(t) = 0 \tag{7}$$

Here, mp and mg are the masses of the pinion and gear; and, ζ_{pSx} and ζ_{gSx} are the damping ratios in the X direction. Likewise, the translational motions $y_p(t)$ and $y_g(t)$ in the Y direction are governed by the following, where ζ_{pSy} and ζ_{gSy} are the damping ratios in the Y direction:

$$m_p \ddot{y}_p(t) + 2\zeta_{pSy}\sqrt{k_{pSy} m_p}\,\dot{y}_p(t) + k_{pSy} y_p(t) - \sum_{i=0}^{n} F_{pfi}(t) = 0 \tag{8}$$

$$m_g \ddot{y}_g(t) + 2\zeta_{gSy}\sqrt{k_{gSy} m_g}\,\dot{y}_g(t) + k_{gSy} y_g(t) - \sum_{i=0}^{n} F_{gfi}(t) = 0 \tag{9}$$

Assumed time-varying mesh stiffness is defined below where t_a represents the time from two teeth in contact to first tooth leaving contact, t_b represents the time from two teeth in contact to the pitch point (subscript b) where the sliding velocity changes its direction and t_c represents the gear mesh period (in time).

$$k(t)=\begin{cases} k_1(t), & 0 \le t < t_a \\ k_2(t), & t_a \le t < t_c \end{cases}, \qquad c(t)=\begin{cases} c_1(t), & 0 \le t < t_a \\ c_2(t), & t_a \le t < t_c \end{cases} \tag{10 a, b}$$

Fig. 2 shows simplified periodic variations in the dimensionless form where . Here the dimensionless mesh stiffness is given by where is the time-averaged operator. The normalized times about which the actual transitions for mesh stiffness from two teeth in contact to first tooth leaving contact take place are given by and , as illustrated in Fig 5.2.

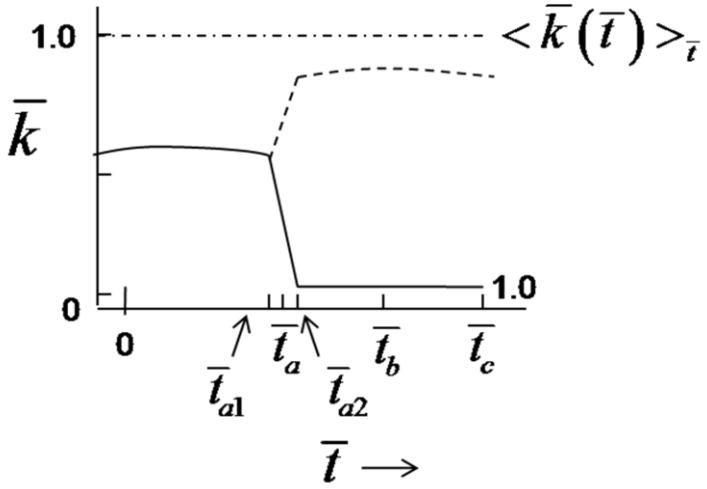

Fig 2. Simplified periodic variations of the Mesh stiffness 6DOF model within one mesh cycle. Key: ——, tooth pair #0; - - - - -, tooth pair #1. Here is the normalized time where , and .

1.2 Acceleration trend prediction from 6DOF model

The 6DOF model predicts the acceleration of gear and pinion along LOA and OLOA in frequency domain. The acceleration value is taken at first 5 gear mesh frequency harmonics for further analysis as these are going to influence the overall acceleration level. The predicted

acceleration value of the pinion and gear along LOA and OLOA direction are calculated at the harmonics for each of the experimental runs

An ANOVA is performed on the acceleration result from the extended 6DOF model at the experimentally measured conditions with torque, speed and finish as main effects and temperature as a covariate. The main effects and two-way interactions (denoted by * between the main effects) were analyzed. Here, the RMS values of the first harmonic of the pinion and gear accelerations in LOA and OLOA direction are taken for the statistical analysis.

The finish, speed, torque and interaction between finish and torque are significant parameters for the acceleration. The average RMS value for each of the test level of the first harmonic of the acceleration with torque and speed are shown in Fig 3(a) and 3(b).

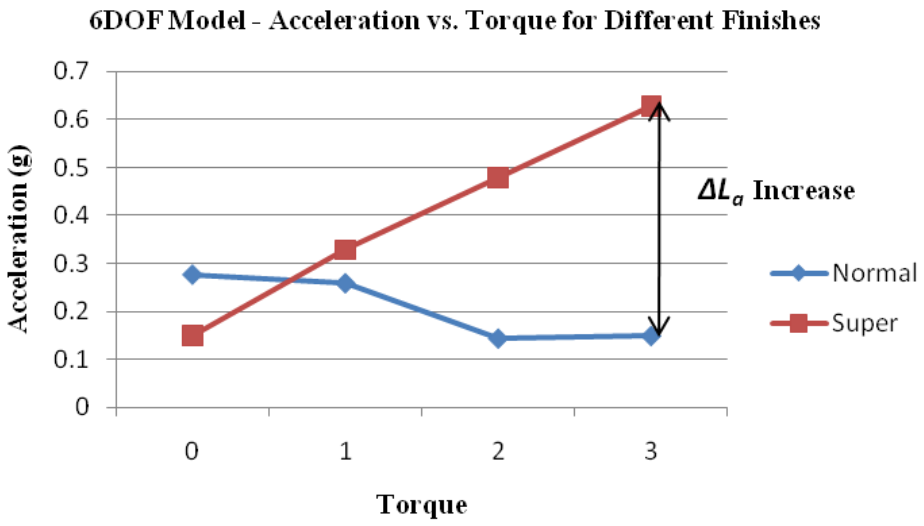

(a)

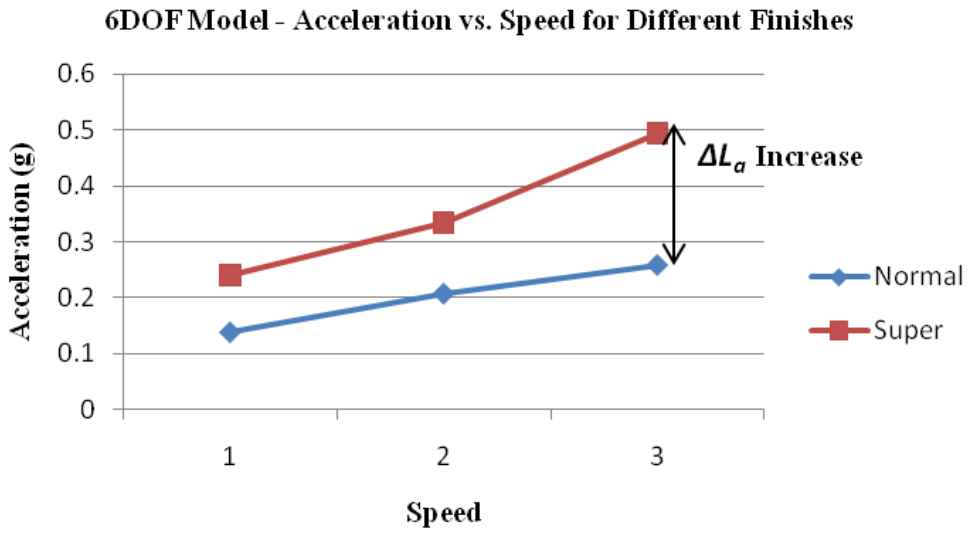

(b)

Fig 3: ANOVA result (a) Variation of RMS of first harmonic of acceleration with torque; (b) Variation of RMS of first harmonic of acceleration with speed

In these plots, the actual torque and speed values are not used. Instead, each torque value is treated as torque level, likewise with speed. From the plots, as torque increases, the acceleration value and ΔL value increase; as speed increases, the acceleration value and ΔL value increase.

2. Experiments conducted on single mesh spiral bevel gear box

Sound pressure and acceleration measurement experiments were conducted on single mesh spiral bevel gear box at the KAC. The measurements were collected with the gear box placed within an acoustically treated enclosure (to soften the environment and effectively improve the measurement strength of the radiated sound pressures from the gear box in comparison to the ambient background noise from the rest of the test rig). In these gear pairs, the gear and the pinion have axes perpendicular to each other. The schematic of the experimental setup is given in

Fig 4.

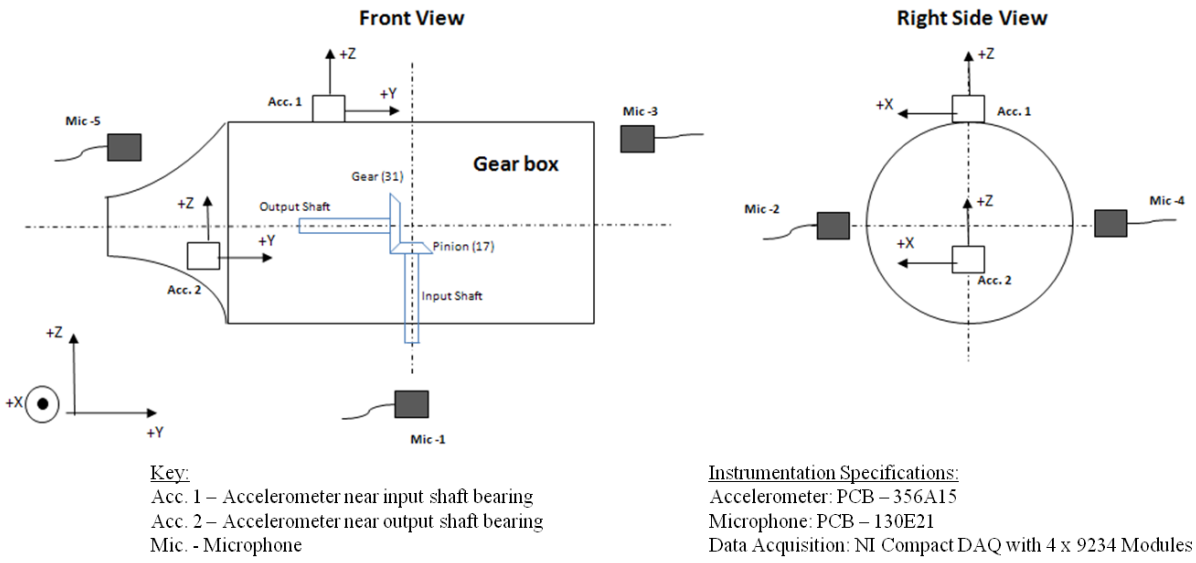

Key:
Acc. 1 – Accelerometer near input shaft bearing
Acc. 2 – Accelerometer near output shaft bearing
Mic. - Microphone

Instrumentation Specifications:
Accelerometer: PCB – 356A15
Microphone: PCB – 130E21
Data Acquisition: NI Compact DAQ with 4 x 9234 Modules

Experimental details

- Input – Pinion, 17 teeth
- Output – Gear, 31 teeth
- Rated input speed – 3061 rpm
- Rated power – 250 hp
- 2 tri-axial accelerometers on the gearbox casing
  - One near input shaft bearing
  - One near output shaft bearing
- 5 microphones mounted in enclosure around the gearbox
- Sound pressure and acceleration data were collected
- Input speed, torque, and oil temperature recorded

Fig 4: Schematic of the spiral bevel gear experimental setup

The experiment consisted of 17 runs at different speeds, torques and temperatures. The first 3 runs were conducted at minimum torque at lower temperature and last two runs were conducted at minimum torque with higher temperature. The gear box casing acceleration and sound pressure autopower spectra were recorded for each run using 100 averages, Hanning window, 3.125 Hz frequency resolution and 12.8 kHz bandwidth. The summarized acceleration and sound pressure values were reported at the harmonics of gear mesh frequency. The same sets of experiments were conducted for gears with normal (before reconditioning) and super finish (reconditioned).

2.1 Results from the experimental runs

The harmonics, the ΔL values are very minimal; indicating that the difference in these levels between the super finish and normal finish gears is minimal. Fig 5 and Fig 6 show the variation of acceleration and sound pressure level with torque and speed.

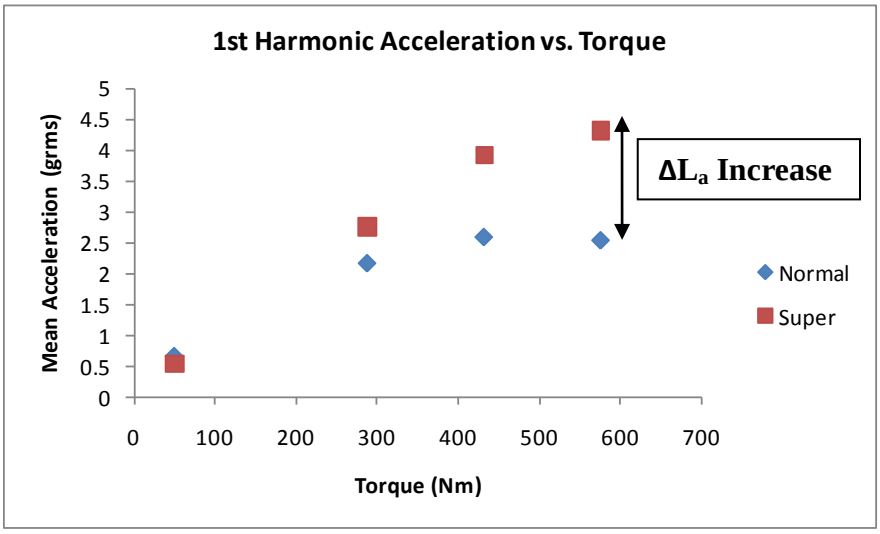

(a)

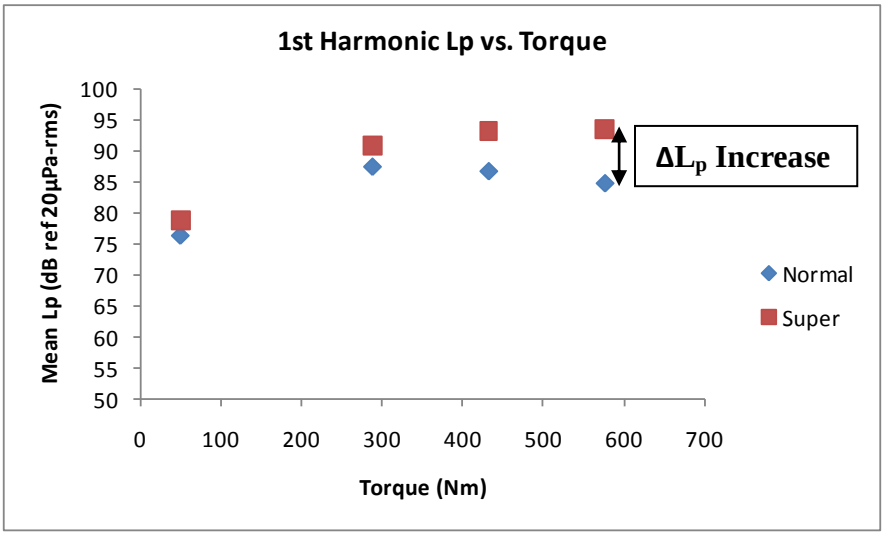

(b)

Fig 5: Trend from ANOVA (a) Acceleration vs. Torque, (b) Sound pressure level vs. Torque

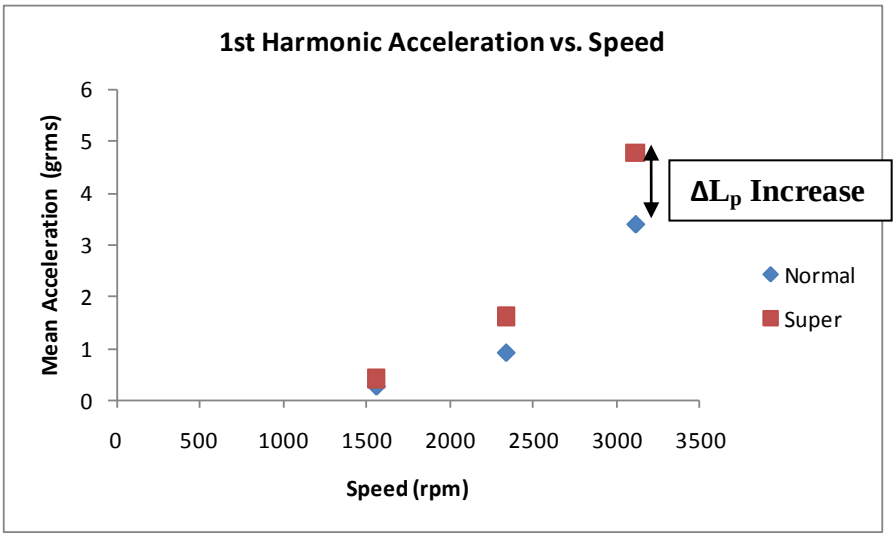

(a)

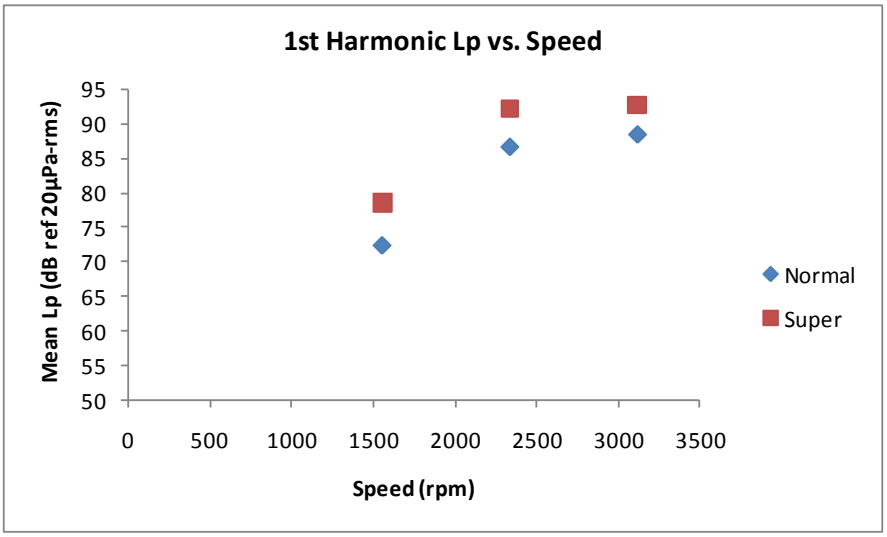

(b)

Fig 6: Trend from ANOVA (a) Acceleration vs. Speed, (b) Sound pressure level vs. Speed

3. Comparison of the acceleration result from the 6DOF model with experimental acceleration result

To compare trends seen in the experimental and modeling results, mass, mass moment of inertia and base radii of both pinion and the gear of 6DOF model are calculated from the experimental spiral bevel gears. The surface undulation height $h_p(t)$ and $h_g(t)$ are taken from an AGMA paper on super finishing by Sikorsky Aircraft Corporation [30]. Static transmission error $\varepsilon(t)$, tooth mesh stiffness ($k_p(t)$ and $k_g(t)$) for pinion and gear are calculated from LDP for different input torques. The tooth profile modification is applied for the normal gear. The super finished gears are assumed to be having an involute profile. The pinion and gear accelerations are calculated along LOA and OLOA direction.

The first harmonic of the acceleration and the sound pressure level from the experimental results are plotted as a variation with torque in Fig 7. In the same plot, the calculated LOA acceleration for pinion and gear are plotted.

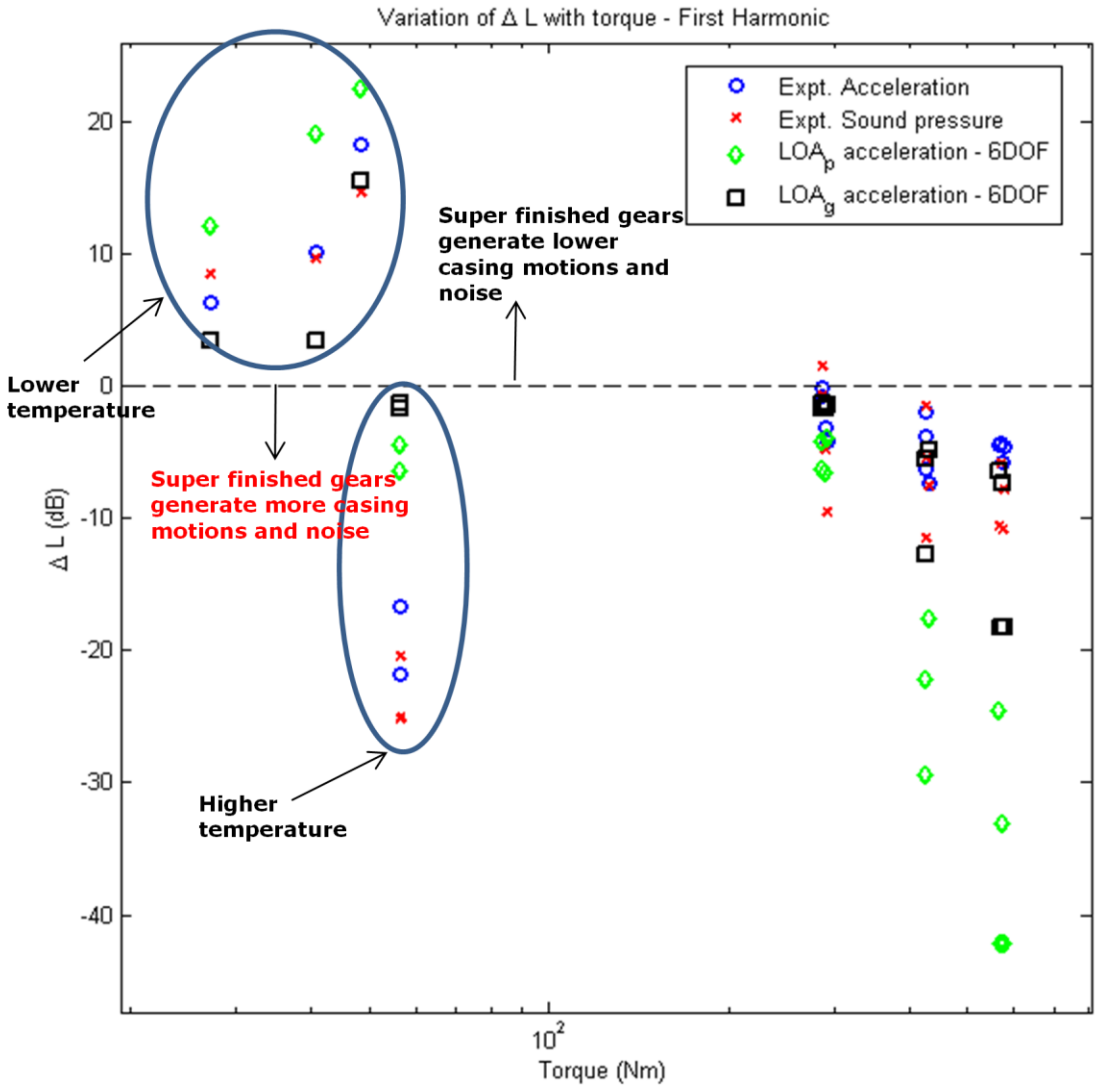

Fig 7: Comparison of ΔL from 6DOF model and experiment; ΔL vs. torque

From the plot, lower torque and temperature on the super finished gears are associated with lower casing motion and radiated noise. At minimum torque and higher temperature, super finished gears produce very high casing motion and noise compared to the normal finished gears. At higher torques (like 50%, 75% and 100% of rated torque), in most cases, the super finished gears produce greater motion and noise, although the ΔL values are low in most cases. The experimental values exhibit similar trends.

In the plot of ΔL vs. speed, shown in Fig 5.8, the acceleration and sound pressure level values obtained from the experiments also show similar trends as the 6DOf model.

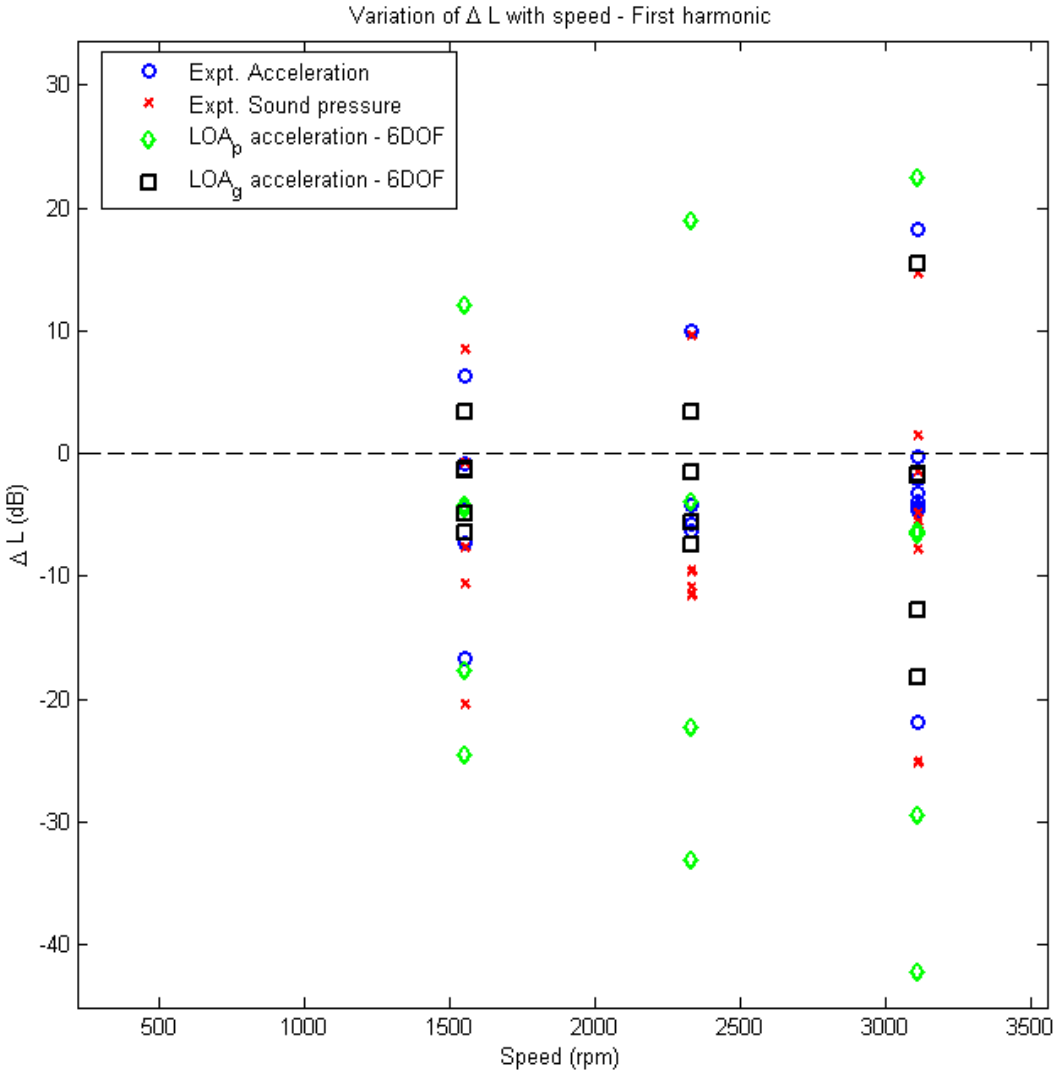

Fig 8: Comparison of ΔL from 6DOF model and experiment; ΔL vs speed

ANOVA results showing the variation of the acceleration with torque is shown in Fig 9 (a) and (b) for 6DOF result and experimental result. In both cases, the difference in acceleration values between the normal and super finish increase with torque, and super finish gears exhibit higher acceleration levels as torque increases.

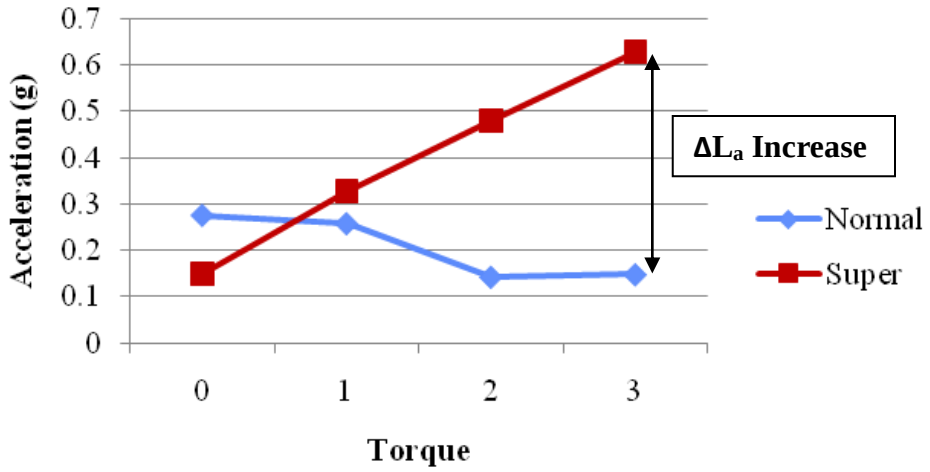

(a)

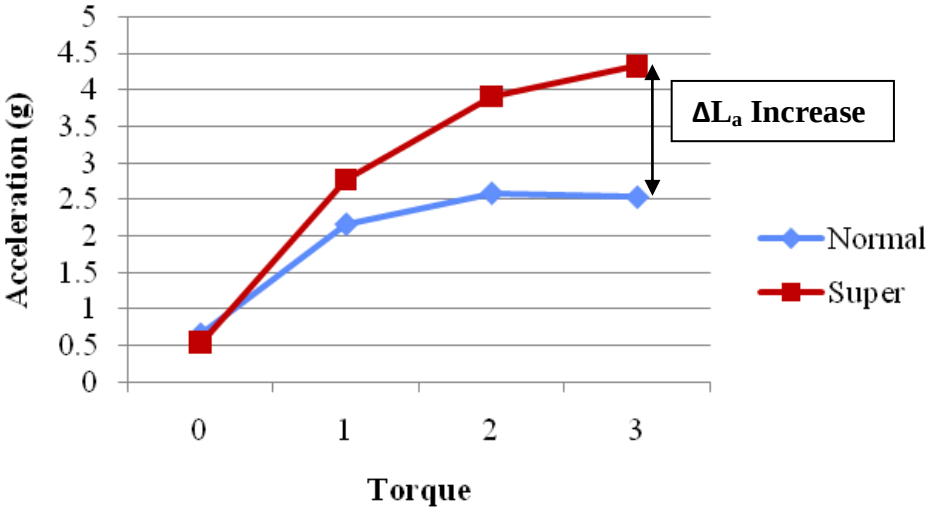

(b)

Fig 9: ANOVA result – Mean acceleration at different levels of Torque; (a) 6DOF model result, (b) Experimental result

ANOVA results showing the mean acceleration level with respect to speed is shown in Fig 10 (a) and (b) for 6DOF result and experimental result. Shown in the plots, increases in speed lead to

increases in acceleration normal and super finished gears according to both the 6DOF model and experimental results. The differences between the acceleration of normal and super finished gears increase with speed in both cases. The experimental result follows the same trend as the 6DOF model result.

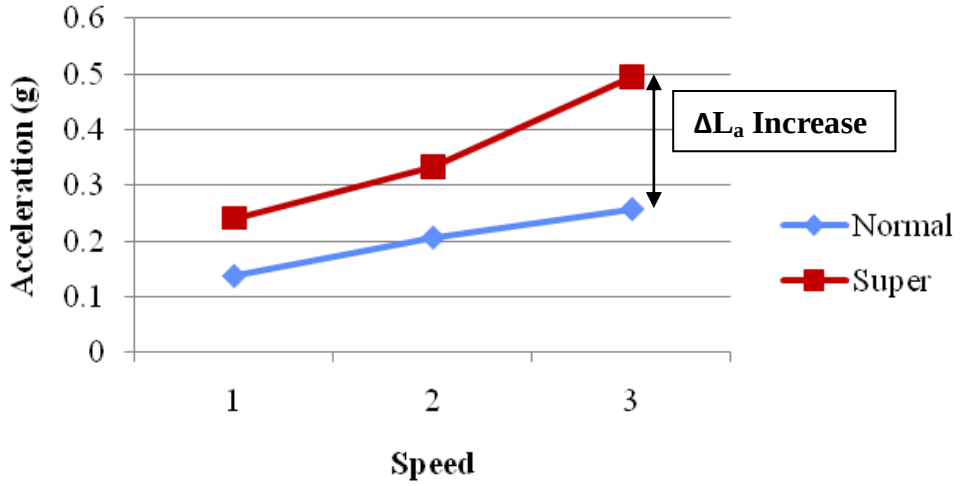

(a)

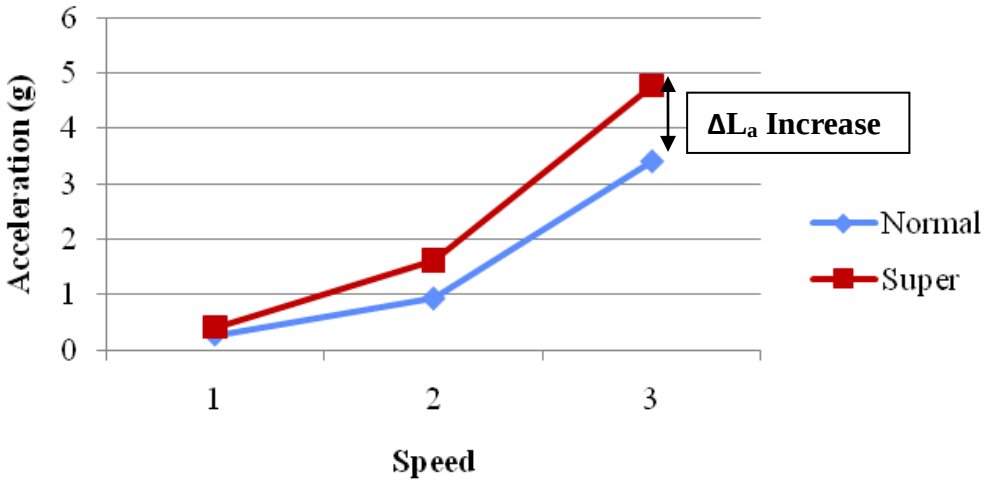

(b)

Fig 10: ANOVA result – Mean acceleration at different levels of speed; (a) 6DOF model result, (b) Experimental result

3. Conclusion

The gear dynamics is studied analytically using lumped system model. It is verified using experiments. It is found that super finishing is effective in reducing the acceleration and noise level only at lower torques. At higher torque, it actually increases the noise level.

4. References

[1] S. He, R. Gunda and R. Singh, Effect of Sliding Friction on the Dynamics of Spur Gear Pair with Realistic Time-Varying Stiffness, Journal of Sound and Vibration, 301, 927-949, 2007.

[2] S. He, R. Gunda and R. Singh, Inclusion of Sliding Friction in Contact Dynamics Model for Helical Gears, ASME Journal of Mechanical Design, 129(1), 48-57, 2007.

[3] M. Vaishya and R. Singh, Strategies for Modeling Friction in Gear Dynamics, ASME Journal of Mechanical Design, 125, 383-393, 2003.

[4] M. Vaishya and R. Singh, Sliding Friction Induced Non-linearity and Parametric Effects in Gear Dynamics, Journal of Sound and Vibration, 248(4), 671-694, 2001.

[5] M. Vaishya and R. Singh, Analysis of Periodically Varying Gear Mesh Systems with Coulomb Friction Using Floquet Theory, Journal of Sound and Vibration, 243(3), 525-545, 2001.

[6] K. F. Martin, A Review of Friction Predictions in Gear Teeth, Wear 49, 201-238, 1978.

[7] K. Ishida and T. Matsuda, Effect of Tooth Surface Roughness on Gear Noise and Gear Noise Transmitting Path, ASME 80-C2/DET-70, 1980.

[8] W. D. Marks, Contributions to the Vibratory Excitation of Gear Systems from Periodic Undulations on Tooth Running Surfaces, Journal of the Acoustical Society of America, 91(1), 166-186, 1991.

[9] S. Kim and R. Singh, Gear Surface Roughness Induced Noise Prediction Based on a Linear Time-Varying Model with Sliding Friction, Journal of Vibration and Control, 13(7), 1045-1063, Jul. 2007.

[10] Mitchell, L. D., 1971, "Gear Noise: the Purchaser's and the Manufacturer's View," Purdue Noise Control Conference, West Lafayette, IN, 95-106.

[11] Kim, S. and Singh, R., 2007, "Gear Surface Roughness Induced Noise Prediction Based on a Linear Time-Varying Model with Sliding Friction," Journal of Vibration and Control, 13(7), 1045-1063.

[12] He, S., Singh, R. and Pavic, G., 2008, "Effect of Sliding Friction on Gear Noise Based on a Refined Vibro-Acoustic Formulation," Noise Control Engineering Journal, 56(3), 164-175

[13] Vaishya, M. and Singh, R., 2003, "Strategies for Modeling Friction in Gear Dynamics," ASME Journal of Mechanical Design, 125, 383-393.

[14] Hansen, B., Salerno, M. and Winkelmann, L., 2006, "Isotropic Superfinishing of S-76C+ Main Transmission Gears," American Gear Manufacturing Association, Paper # 06FTM02.

[15] Amini, N. and Rosen, B. G., 1997, "Surface Topography and Noise Emission in Gear boxes," ASME Design Engineering Technical Conferences, Paper # DETC97/VIB-3790.

[16] Load Distribution Program (LDP), Windows 3.3.0 version, 2009, Gear and Power Transmission Research Lab, The Ohio State University.

[17] CALYX software, 2002, A contact mechanics/finite element (CM/FE) tool for spur gear design, ANSOL Inc. <www.ansol.com>, Hilliard, OH.

[18] Houlob, A., 2005, ”Mobility analysis of a spur gear pair and the examination of sliding friction,” MS Thesis (Advisor: R. Singh), The Ohio State University.

[19] Karthik, J., 2010, “Structure-borne Noise Model of a Spur Gear Pair with Surface Undulation and Sliding Friction as Excitation,” MS Thesis, The Ohio State University.